Applied Acoustics 102 (2016) 49–54

Contents lists available at ScienceDirect

Applied Acoustics

journal homepage: www.elsevier.com/locate/apacoust

Design of metaporous supercells by genetic algorithm for absorption optimization on a wide frequency band

C. Lagarrigue *, J.-P. Groby, O. Dazel, V. Tournat

LUNAM Université, Université du Maine, CNRS, LAUM UMR 6613, Av. O. Messiaen, 72085 Le Mans, France

ARTICLE INFO

Article history:
Received 16 January 2015
Received in revised form 25 August 2015
Accepted 10 September 2015

Keywords:
Metamaterials
Porous materials
Metaporous
Finite element method
Genetic algorithm optimization

ABSTRACT

The optimization of acoustic absorption by metaporous materials made of complex unit cells with 2D resonant inclusions is realized using genetic algorithm. A nearly total absorption over a wide frequency band can be obtained for thin structures, even for frequencies below the quarter wavelength resonances i.e., in a sub-wavelength regime. The high absorption performances of this material are due to the interplay of usual visco-thermal losses, local resonances and trapped modes. The density of resonant and trapped modes in this dissipative porous layer, is a key parameter for broadband absorption. The best configurations and critical coupling conditions are found by genetic algorithm optimization. Several types of resonators are included gradually in the studied configurations (split-rings, Helmholtz resonators, back cavities) with increasing complexity. The optimization leads to a metaporous structure with a 2-cm sub-wavelength layer thickness, exhibiting a nearly total absorption between 1800 Hz and 7000 Hz. The influence of the incidence angle on the absorption properties is also shown.

1. Introduction

Acoustic porous materials are widely used in noise control applications for their interesting sound absorbing properties in the middle and high frequency ranges (>1000 Hz) but they suffer from a lack of efficiency at lower frequencies [1]. These last decades, several ways to avoid the problem of absorption in the low part of the audible frequency range (<1000 Hz) have been proposed. The generally implemented solutions make use of multi-layer packages. This solution has limits at low frequencies while trying to keep the thickness of the treatment relatively small compared to the incident wavelength that has to be absorbed. Recently, new directions have been explored, based on combining resonant and scattering phenomena with the traditional viscous and thermal losses. Whatever the frequency is, the key is to excite modes of the structure that will trap the energy inside it for a long time and therefore enhance the absorption of the whole structure. Among different studied configurations, i.e., double porosity [2,3], dead-end porosity [4], multiple scattering [5], we focus here on configurations composed of periodic rigid inclusions and resonant inclusions embedded in a porous layer (often refereed as metaporous materials) [6–8].

The effect on the absorption properties of a periodic embedment of both non-resonant and resonant inclusions in a porous layer has been studied in two (or three) dimensions, when the porous layer is either backed by a rigid backing [6–9], possibly incorporating cavities [10], or radiating in a semi-infinite half-space [11] in the case of transmission problems. Different inclusion shapes have been studied [6,7,12,13] showing similar results at low frequencies. The enhanced absorption compared to simple porous media has been explained by the coupling of several phenomena: scattering by periodic inclusions and/or back cavities local resonances that trap the energy inside the inclusions or cavities, excitation of a localized mode that traps energy between the rigid backing and the inclusions, and excitation of the modified mode of the backed layer similar to Wood's anomaly. The rigid backing acts as a perfect mirror and allows interaction between the inclusion and its image to excite the trapped mode [6]. In these previous studies, the relatively simple configurations allowed for some analytical and semi-analytical modeling, together with numerical simulations and experiments. Consequently, the observed effects of perfect absorption (i.e. the absorption coefficient is 1), or nearly perfect absorption (the absorption coefficient is close to 1) for narrow frequency bands could be interpreted and associated to specific processes. The dependencies of the absorption properties on the metaporous cell parameters (such as the inclusion shape, size, position, and resonance frequency) could be interpreted and in some cases predicted and tailored.

* Corresponding author.
E-mail address: clement.lagarrigue@univ-lemans.fr (C. Lagarrigue).

http://dx.doi.org/10.1016/j.apacoust.2015.09.011
0003-682X/

Table 1
Supercells geometric parameters range values.

x_i (mm)	y_i (mm)	ϕ_i (rad)	r_i (mm)	e_i (%)
[4; 16]	[4; 16]	[0; 2π]	[2; 10]	[10; 90]

Table 2
Parameters used for the routines.

Routine	Selection	Mutation	Crossover	Sharing	Scaling
Type	Roulette	Multipoint	Non-uniform	Large exploration	Exponential
Parameter		3	$b = 1$	$\alpha = 0.8$ $\sigma = 0.95$	$q = 1$

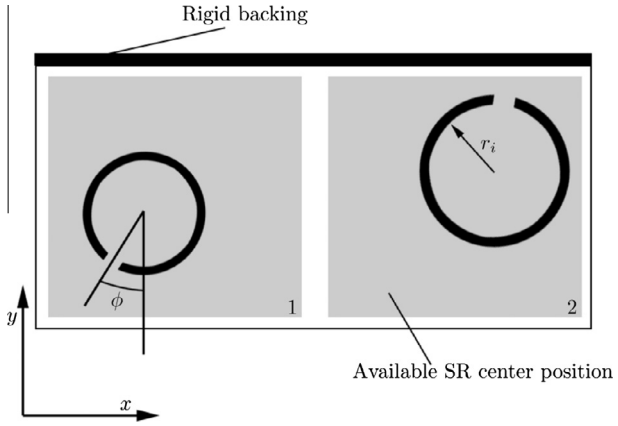

Fig. 1. Outline of a random unit cell.

Table 3
Parameters of the porous foam used in the article.

ϕ	α_∞	Λ (μm)	Λ' (μm)	σ (N s m^{-4})	f_v (Hz)
0.95	1.42	180	360	8900	781

In the present article, we propose a way to design metaporous materials able to strongly absorb the incident acoustic energy over a wide frequency band, for wavelengths in air larger than the material thickness. As mentioned previously, the density of modes trapping the energy inside the layer should be large enough in the frequency range of interest, which requires complex metaporous unit cells (or super-cells). The number of parameters defining the metaporous super-cell can consequently become large (all geometrical parameters of the inclusions and back cavities, parameters of the porous medium) and the effect of varying one of them on the absorption properties is unpredictable due to the influence on several coupled or competing absorption processes. In particular, the perfect absorption condition which can be analytically found in some configurations defined by only few parameters (see e.g. the one-dimensional case of a weakly lossy resonator, critically coupled to a waveguide cavity in [14], or the two-dimensional case of membrane resonator panel in [15]) is impossible to predict in the case of metaporous two-dimensional and three-dimensional super-cells composed of several resonators, back cavities and a porous material with frequency dependent acoustic properties. Therefore, in order to find metaporous super-cell configurations having high and broadband absorption, we make use of Genetic Algorithm (GA) optimization. In other words, we find empirically the metaporous super-cell parameters such that the different wave processes (scattering, trapped modes, local resonances and critical coupling, frequency dependent wave dissipation...) play together for high and broadband absorption.

The configuration analyzed in the following is composed of an infinite periodic set of two-dimensional (2D) metaporous super-cells. Each super-cell can contain 2D resonant inclusions embedded in a porous layer which is backed by a hard wall with or without resonant cavities. For the sake of clarity and to analyze the influence of each elements, we decided to make an incremental study where the complexity of the super-cells increases by the successive addition of ingredients. The optimization by the in-home genetic algorithm code begins with a previous configuration analyzed in [8] and evolves to account for more resonators per super-cells and a larger number of degrees of freedom.

2. Optimization by genetic algorithm

The genetic algorithm is set to find the configuration having the highest acoustic absorption in average over 80 points on the frequency range from 100 Hz to 7 kHz.

The geometry of the problem is two-dimensional and periodic, the inclusions being split-rings and 2D Helmholtz resonators and the cavities being 2D. The problem therefore reduces to the solution of the pressure field in the unit cell because of the periodicity and excitation by a plane incident wave. Bloch-Floquet conditions are applied to the left and right boundaries to consider the infinite periodicity as explained in [16]. For this to be correctly implemented, the two sides were discretized with similar nodes, i.e. identical vertical coordinates. All simulations are performed by considering a normal incident wave arising from a semi infinite space to the bottom of the cell. The top of the cell is considered perfectly rigid (Neumann type boundary condition). All the geometrical parameters are chosen by the algorithm except two: the thickness (20 mm) of the plate and the spatial periodicity (40 mm). The other parameters (summarized in Table 1) are set in a range of values that allow almost all configurations: where $i = 1$ or $2, x_i$ and y_i are respectively the longitudinal and the vertical position of the inclusion i, ϕ_i is the angular position of the slit, the origin is chosen centered on each inclusion and the direction is $-y, r_i$ is the internal radius of the inclusion and e_i is the thickness.

The program is coded in Fortran and uses classical minimum search (selection, mutation and crossover [17,18]) and fast convergence (sharing, scaling and elitism [17,19]) routines. Because of the possible high number of parameters, these routines are configured

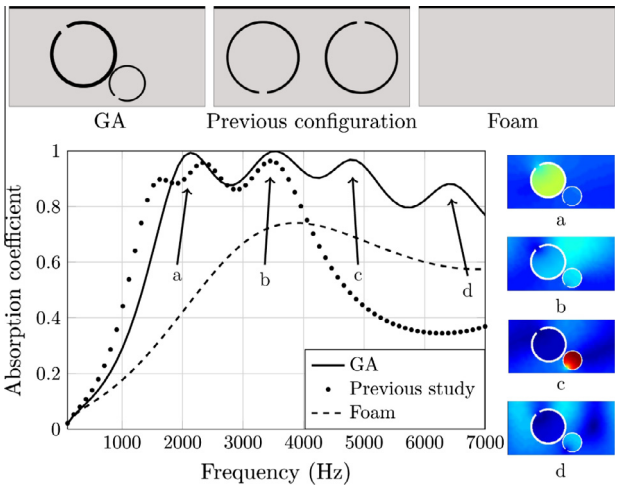

Fig. 2. Absorption coefficient for a super-cell composed of two split-rings.

Table 4
Geometric parameter values for the first optimization results called GA.

x_1 (mm)	x_2 (mm)	y_1 (mm)	y_2 (mm)	ϕ_1 (rad)	ϕ_2 (rad)	r_1 (mm)	r_2 (mm)	e_1 (mm)	e_2 (mm)
15	24	10	5	1.25π	22	7	4	0.85	0.75

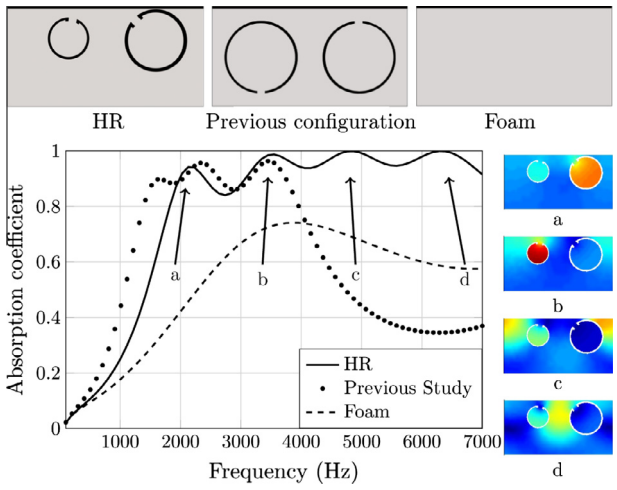

Fig. 3. Absorption coefficient for a supercell composed of two 2D Helmholtz resonators.

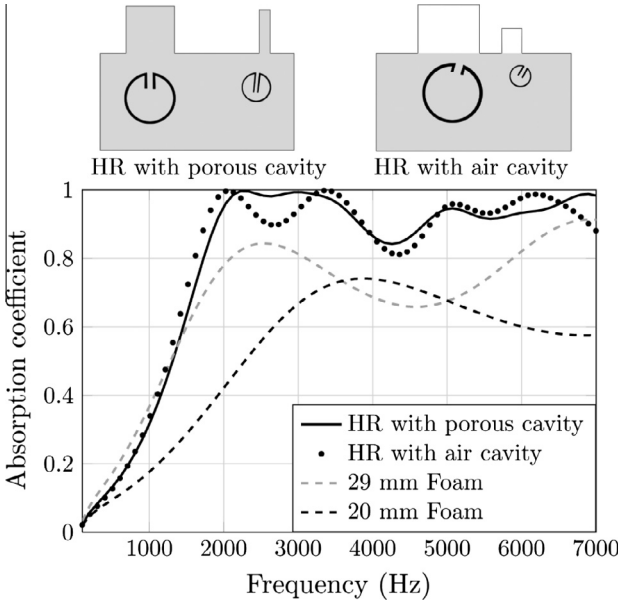

Fig. 4. Absorption coefficient for a supercell composed of two 2D Helmholtz resonators and two cavities.

to ensure a large exploration of the possibilities. All the types of routines and factors used are summarized in Table 2.

During an iteration of the optimization process, a population is set with different geometry parameters, then each individual acoustic response is simulated with a Finite Element Method (FEM) program. This program has been developed and validated in [16,6,8] and uses the open source software FreeFem++ to mesh each configurations. Linear finite elements are used to approximate the pressure inside the unit cell, thereby leading to a discretized problem of 1500 elements and 800 nodes. The porous mesh is configured to be adaptive and to always have elements 10 times smaller than the smallest wavelength in air ($\lambda = 5$ cm for 7 kHz in this case). The mesh is refined in the inclusion opening to ensure a good discretization of the pressure field. For each individual, the size and the number of mesh elements are recalculated according to the size of the inclusions. The optimization is done by comparing each absorption coefficient and by choosing the best geometries for the next iteration. The implemented porous model is an equivalent fluid where the effective density is modeled by the Johnson et al. model [20] and the bulk modulus by the Champoux–Allard model [21]. The inclusions are considered rigid. The FEM program gives the absorption coefficient as:

$$A(j) = 1 - \sum_q \frac{Re(k_{2q})}{k_{20}^i} |R_q(j)|^2 \tag{1}$$

with $R_q(j)$ the reflexion coefficients of the qth Bloch-wave for the frequency j, k_{2q} the Bloch-wavenumber along the normal incidence and k_{20}^i the incident plane wave.

Here, the fitness [17,18] is linked to the absorption coefficient averaged over the considered frequency range and defined such as $f_i = 1 - \alpha_i$, where

$$\alpha_i = \frac{1}{n_{freq}} \sum_{j=1}^{n_{freq}} A(j), \tag{2}$$

with n_{freq} the number of frequencies of the absorption coefficient calculated by the FEM code. To avoid optimization results providing non-realistic geometries, the GA needs to be constrained. The solution chosen here is to make the list of all non-realistic solutions (overlapping inclusions for example) and to penalize the fitness if the GA chooses one of them (if non-realistic solution: $f_i = 1, f_i = 1 - \alpha_i$ else). All simulations are done with populations of 30 individuals and 1000 generations to ensure a good convergence of the results.

The genetic algorithm is first used to optimize a metaporous, whose unit cell is composed of a porous plate (fireflex©, Recticel©, a porous material widely used for its good acoustic and fire resistant properties) backed with a rigid wall and two resonant inclusions. Fig. 1 depicts one of the unit cell analyzed during the optimization process and Table 3 gives porous matrix parameters.

With σ the static flow resistivity, α_∞ the tortuosity, ϕ the porosity, Λ the viscous characteristic length, Λ' the thermal characteristic length and f_v the Biot frequency.

Table 5
Geometric parameters values for the second optimization results called HR.

x_1 (mm)	x_2 (mm)	y_1 (mm)	y_2 (mm)	ϕ_1 (rad)	ϕ_2 (rad)	r_1 (mm)	r_2 (mm)	l_1 (mm)	l_2 (mm)
12.5	30	14	13.5	0.91π	1.25π	4	6	0.1	0.14

Table 6
Geometric parameters values for the optimizations with HR and back cavity.

Inclusions	$x1$ (mm)	x_2 (mm)	y_1 (mm)	y_2 (mm)	ϕ_1 (rad)	ϕ_2 (rad)	r_1 (mm)	r_2 (mm)	l_1 (mm)	l_2 (mm)
HRC1	10	32	10.5	13	π	0.91π	5	3	1.2	1
HRC2	10.5	24.5	12	15.5	1.08π	1.16π	6	2	1.2	1.6
Cavity	h_1 (mm)	h_2 (mm)	w_1 (mm)	w_2s(mm)	x_1 (mm)	x_2 (mm)				
HRC1	9.8	9	10	2	15	35				
HRC2	10	5	12.5	4	14	31				

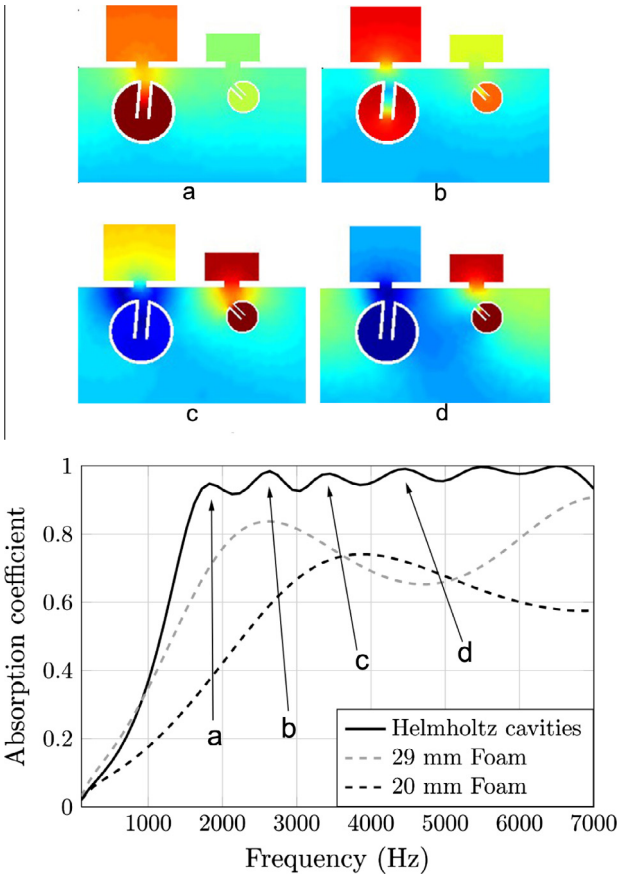

Fig. 5. Absorption coefficient for a supercell composed of two 2D HR and two Helmholtz air cavity.

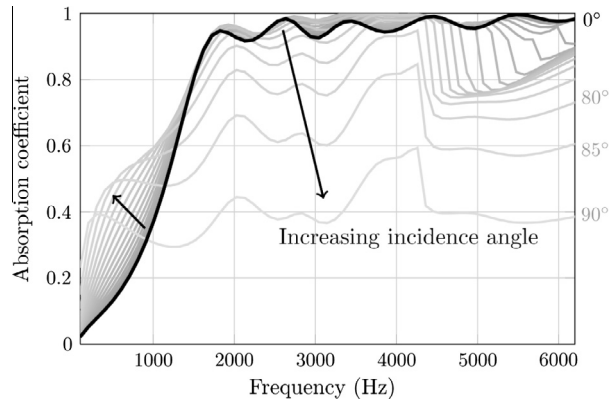

Fig. 6. Comparison of the absorption coefficient in function of the incidence angle.

3. Optimization results

Compared to the previously studied configurations [8], the split-ring positions, radii and split-ring thicknesses are here optimized by the GA. Fig. 2 shows a comparison of the results of a first optimization, the previously proposed unit cell and the foam without any inclusion. GA results (dimensions summarized in Table 4) exhibit a very good enhancement of the absorption properties with a fitness of 0.25 while the unit cell of the previous configuration has a fitness of 0.42 and the foam alone 0.41. In the GA optimized cell, the two inclusions are almost in contact. It is still manufacturable by inserting these two inclusions in contact, or by considering only one inclusion with this special shape manufactured with a 3D printer.

In Fig. 2 two different localized modes are observed: at 3500 Hz, snapshot (b) and at 6500 Hz snapshot (d), that trap the energy between the rigid backing and the inclusions. The two other peaks are clearly due to the resonance of the inclusions (snapshot (a) and (c)). The addition of this four phenomena leads to the absorption enhancement over the frequency band considered. Even if the absorption coefficient of the GA results is lower than the previous study in the lowest frequency range, it does not exhibit the Bragg effect around 6 kHz. This effect appears in periodic media when the periodicity is half wavelength of the incident wave [22]. In here, it is related to the distance between the inclusion and its image with respect to the rigid backing. Here it is minimized by tuning the resonance effects near this frequency (the resonance of an inclusion snapshot (c) and a localized mode snapshot (d)).

Unfortunately, these resonance frequencies are all related to the size and position of the inclusions and it is not possible to reach a larger absorption coefficient at low frequency without considering split-rings larger than the thickness of the plate. This possibility is not compatible with our constrain of fixed thickness. To try to solve this problem, a neck is added to the split-rings to lower the resonance frequency and to add another degree of freedom in the GA. This type of inclusion is called in this paper 2D Helmholtz Resonator or 2DHR (see Fig. 3).

The results are close to the first simulation with a fitness of 0.24. The absorption coefficient is now lower below 2600 Hz but larger elsewhere, in particular near the Bragg frequency where it has completely vanished. These results are different from what we where expecting by using inclusions that can have lower resonance frequencies but changing resonances for the low frequency range, would have destroyed the absorption coefficient elsewhere resulting in a much higher fitness (see Table 5).

Another way to overcome this limit is to add air filled back cavity. They can act as quarter wavelength resonators but must be very long in comparison to the dimension of the plate to have a sufficiently low resonance frequency and this is also out of the scope of this article. However, these cavities can be curved allowing to make a ultra thin low frequency sound absorbing panels based on coplanar spiral tubes or coplanar Helmholtz resonators [23].

The initial goal of enhancing the absorption coefficient below the Biot frequency with the inclusions or with the back cavities

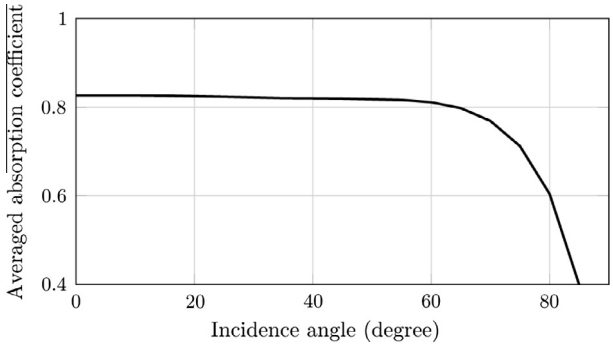

Fig. 7. Averaged absorption coefficient in function of the incidence angle.

is aborted because of this dimensions constraint. Now cavities are still added, but with reasonable dimensions (less that the thickness of the plate) to add more resonances and to keep the absorption coefficient near 1 over a larger frequency range. The rigid backing is now modified and present two rectangular cavities per spatial period. Two other runs are performed, one with the cavity filled with the same porous media and a second one with a cavity filled with air (see Fig. 4).

These two results (dimensions are summarized in Table 6) present respectively a fitness of 0.22 and 0.21 that are better than the previous one(s). The absorption coefficient is compared with the one of the two corresponding homogeneous layer thicknesses: 20 mm and 29 mm. This last value corresponds to the total thickness of the porous plate + cavity. The absorption coefficient now reaches 1 near 2000 Hz and stays close to unity for higher frequencies, except near 4200 Hz. In this simulations, the GA tends to place again the inclusions in front of the cavity, with the slit facing the back cavity. This results in the excitation of coupled modes between one inclusion and one cavity and gives rise to the absorption coefficient for frequencies lower than the resonance frequency of both elements. For example, in case of a unit cell with air cavity, a coupled mode is excited at 1800 Hz whereas the split-ring resonance is near 2400 Hz. This phenomenon is developed in the next simulation. As expected, even with these optimizations the metaporous cannot reach high absorption at very low frequency. There is clearly a limit at 1500 Hz due to the Biot frequency ($f_v = 781$ Hz for Fireflex material). Below this value, the acoustic propagation is described by a diffusion equation, that cannot allow the HR (filled with porous material) to resonate. Thus, below this frequency, this kind of resonators are of poor interest, unless the porous inside is removed. In this case, the resonance frequency will increase and this will not be interesting anymore for our application.

The next simulations consider a similar configuration as before with air filled back cavities and partially closed openings. This allows to lower the resonance frequency of the cavities because it is now considered as an Helmholtz resonator.

This optimized geometry reaches a fitness of 0.17, which is the best metaporous that can be obtained here. The frequency band of high absorption is now close to unity from 1600 Hz to 7000 Hz with the same thickness than previously (2 cm layer thickness and 9 mm of depth back cavity). The phenomenon of interaction between two elements is clearly visible. At 1600 (snapshot a of Fig. 5) the left HR and the left cavity resonate together and a high pressure zone is clearly visible between them. This exhibits a coupled mode and lower the resonance frequency of the ensemble (same phenomenon at 3400 Hz, snapshot c for the right inclusion and cavity). At 2800 Hz (snapshot b) of Fig. 5) the two elements resonate again but this time, the pressure is localized inside each resonator (same phenomenon at 4500 Hz, snapshot d). This mean that they resonate at their own resonance frequency.

Geometries depicted here are also efficient for other incidence angle. In Fig. 6 only the results of simulation for the last geometry are plotted but the other exhibit the identical behavior. The figure shows the absorption coefficient for incidence angles from 0° (normal incidence, the black curve) to 90° (grazing incidence, gray curves). This is summarized in Fig. 7 where the averaged absorption coefficient over the frequency is plotted in function of the incidence angle. These figures show that the absorption coefficient remains large for a wide range of angle incidence (from 0° to 75°) and only decreases near the grazing incidence. This means that only optimizing for the incidence angle is acceptable to design geometries efficient for diffuse field.

The absorption increases at low frequency when the incidence angle increases because the incident wave propagate over a longer distance to reach the rigid backing and being reflected. Other phenomena are not angle dependent like the inclusions or back cavities resonances and can be always excited.

4. Conclusion

Absorption by metaporous materials is driven by several processes, local resonances, localized mode excitation and mode couplings. It is difficult to tune all of these processes to tailor a high absorption over a wide frequency band because it requires complex geometry super-cells with numerous and interconnected geometrical degrees of freedom. We have successfully used a genetic algorithm to find nearly perfect absorption conditions over a frequency band of 100–7000 Hz: it appears that for a 2-cm thick layer, it is possible to have an almost unity absorption band from 1800 Hz to 7000 Hz by using split-rings (with necks) and back cavities. It is also shown that this optimized unit cell is efficient for non normal incidence angles and provides a good absorption even for incidence angles close from the grazing one. This study only focuses on super-cells with a couple of resonators but there are numerous configurations that could be advantageous. In particular, Helmholtz resonators filled with air (instead of porous medium) could lead to resonances with moderate quality factors below the porous medium Biot frequency, which is not possible with porous filled resonators. If the neck is sufficiently long, it is possible to obtain an arbitrary low resonance frequency and improve even more the absorption properties at long wavelengths.

References

[1] Allard J-F, Atalla N. Propagation of sound in porous media: modelling sound absorbing materials. Chichester: John Wiley & Sons; 2009 [chapter 5].
[2] Olny X, Boutin C. Acoustic wave propagation in double porosity media. J Acoust Soc Am 2003;114:73–89.
[3] Auriault J, Boutin C. Deformable porous media with double porosity iii: acoustics. Trans Porous Media 1994;14(2):143–62.
[4] Dupont T, Leclaire P, Sicot O, Gong X, Panneton R. Acoustic properties of air-saturated porous materials containing dead-end porosity. J Appl Phys 2011;110:094903.
[5] Tournat V, Pagneux V, Lafarge D, Jaouen L. Multiple scattering of acoustic waves and porous absorbing media. Phys Rev E 2004;70:026609.
[6] Groby J-P, Duclos A, Dazel O, Boeckx L, Kelders L. Enhancing absorption coefficient of a backed rigid frame porous layer by embedding circular periodic inclusions. J Acoust Soc Am 2011;130:3771–80.
[7] Nennig B, Renoux Y, Groby J-P, Aurégan Y. A mode matching approach for modeling two dimensional porous grating with infinitely rigid or soft inclusions. J Acoust Soc Am 2012;131:3841–52.
[8] Lagarrigue C, Groby J, Tournat V, Dazel O, Umnova O. Absorption of sound by porous layers with embedded periodic arrays of resonant inclusions. J Acoust Soc Am 2013;134(6):4670–80.
[9] Groby J-P, Lagarrigue C, Brouard B, Dazel O, Tournat V, Nennig B. Using simple shape three-dimensional rigid inclusions to enhance porous layer absorption. J Acoust Soc Am 2014;136(3):1139–48.
[10] Groby J-P, Duclos A, Dazel O, Boeckx L, Lauriks W. Absorption of a rigid frame porous layer with periodic circular inclusions backed by a periodic grating. J Acoust Soc Am 2011;129:3035–46.
[11] Groby J-P, Wirgin A, Ogam E. Acoustic response of a periodic distribution of macroscopic inclusions within a rigid frame porous plate. Waves Random Complex Media 2008;18:409–33.

[12] Lagarrigue C, Groby J-P, Tournat V, Dazel O. Parametric study of a metaporous made of inclusions embedded in a rigid frame porous material glued on a rigid backing. In: Proc of acoustics 2012; 2012 [hal-00810737].
[13] Hyun H, Siu-Kit L. Effects of inclusion shapes within rigid porous materials on acoustic performance. In: 164th meeting of the acoust soc Am, Kansas City, vol. 132; 2012. p. 1905.
[14] Romero-García V, Theocharis G, Richoux O, Merkel A, Tournat V, Pagneux V. Perfect and broadband acoustic absorption by critical coupling. Available from: 1501.00191.
[15] Ma G, Yang M, Xiao S, Yang Z, Sheng P. Acoustic metasurface with hybrid resonances. Nat Mater 2014;13(9):873–8. <http://dx.doi.org/10.1038/nmat3994>.
[16] Allard J, Dazel O, Gautier G, Groby J, Lauriks W. Prediction of sound reflection by corrugated porous surfaces. J Acoust Soc Am 2011;129:1696.
[17] Goldberg D. Genetic algorithms in search, optimization, and machine learning. 1st ed. Addison-Wesley Professional; 1989.
[18] Spears WM, De Jong KA. An analysis of multi-point crossover; 1991. p. 301–15.
[19] Michalewicz Z. Genetic algorithms + data structures = evolution programs. Springer; 1998.
[20] Johnson D, Koplik J, Dashen R. Theory of dynamic permeability and tortuosity in fluid-saturated porous media. J Fluid Mech 1987;176(1):379–402.
[21] Champoux Y, Allard J. Dynamic tortuosity and bulk modulus in air-saturated porous media. J Appl Phys 1991;70(4):1975–9.
[22] Joannopoulos J. Photonic crystals: molding the flow of light. Princeton Univ Pr; 2008 [chapters 5 and 10].
[23] Cai X, Guo Q, Hu G, Yang J. Ultrathin low-frequency sound absorbing panels based on coplanar spiral tubes or coplanar Helmholtz resonators. Appl Phys Lett 2014;105(12):121901.